Inductive Coupling Matrix of a Multiconductor System for a Winding-on-Core Prototype

Fadi Abdallah, Mats Alaküla
Division of Industrial Electrical Engineering and Automation (IEA),
Lund Institute of Technology (LTH), Lund University, P.O. Box 118, SE-221 00 Lund, Sweden
E-mail: fadi.abdallah@iea.lth.se

Abstract— **Broadband circuit models for electric machines are effective means to understand, predict, and control the phenomenon of conducted Electromagnetic Interference (EMI) from immunity/susceptibility perspective. These models should cover the capacitive and inductive coupling behavior of the component along the frequency range of interest. Circuit models used under generic SPICE simulation softwares are very helpful for design-related and troubleshooting activities. In this paper the inductive coupling for a winding on a laminated ferro-magnetic core prototype has been investigated and analyzed with the aid of freely-available FEMM software package.**
Inductive coupling analysis resulted in the generation of a complex-numbered inductive coupling matrix expressing a certain wiring arrangement. This is achieved by automatically generating the desired geometry and assigning boundary conditions for the problem under FEMM through Lua scripting language and then solving for magneto-static and time-harmonic magnetic cases for both self- and mutual- inductances for every conductor in the multi-conductor system. Post-Processing of the solutions is performed and the results are linked back to MATLAB® and stored in a matrix format.
The inductive coupling of the winding turns, along with the capacitive coupling, forms the resulting SPICE circuit model which is compared against prototype measurements taken by Rhode & Schwarz (R&S®) vector network analyzer.

Keywords— Electromagnetic Interference (EMI); Conducted Emissions; Inductive Coupling; Common-mode Voltage/Current; Circuit Simulation Software.

I. INTRODUCTION

Conducted and radiated Electromagnetic Interference (EMI) emission is the downside of increased power density and decreased size and losses for power electronics systems. Pulse-Width Modulation (PWM)-inverter-fed machines inherently result in Common-Mode (CM) voltage [2][10][11][12]. On the other hand, parasitic capacitances-to-ground exist literally all over the vehicular electric drive system [6], as shown in Fig.1. Not least within the electric machine windings and between the winding and the machine core. Parasitic capacitances are usually of low orders of magnitude which make them negligible at low frequency analysis. These capacitances interact with the high-frequency CM voltage waveform and can provide a low-impedance path for the leakage current.

Capacitive impedance path depends on the combination of capacitance value and CM voltage frequency but also on the inductive coupling between winding turns. The high-frequency leakage current takes the form of a damped sinusoid at every instant a change in the varying 2-step/3-step CM voltage waveform occurs [11].

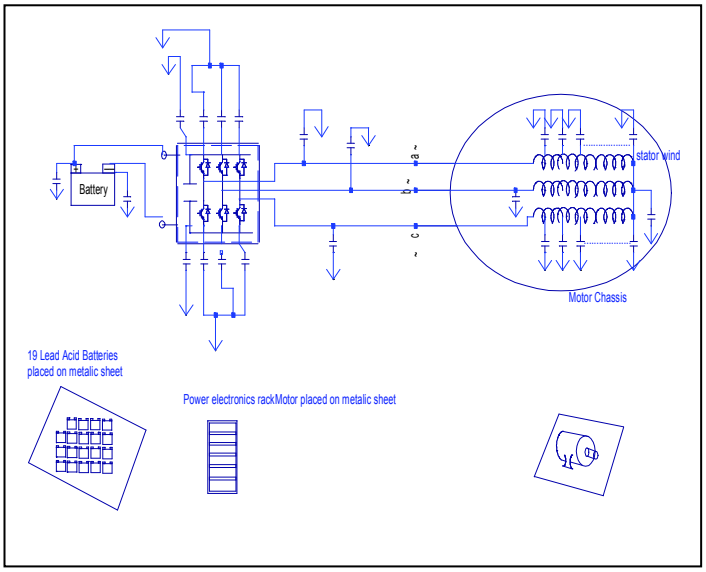

Fig. 1. Parasitic capacitances in an electric drive system

II. TURN-TO-TURN APPROACH

A. Analysis Tools

FEMM and LTspice® along with MATLAB® are used as a complete analysis package for this work. This combination is used to draw the desired geometry, perform Finite Element Method (FEM) analyses, store results in arrays and structure arrays (structs), establish agreement between FEMM outcome and SPICE models and finally propose models and validate them to measurements.

B. Machine Stator Slot

The turn-to-turn analysis level is adopted in modeling the winding portion in a machine stator slot [1][7][9]. Due to the large number of turns, it is significant to automate the modelling process.

C. Simple Winding-on-Core Prototype

An electric machine winding is substituted by a simple winding on an iron core prototype. The prototype has 24 turns and 3 layers, in condensed and spaced wire arrangements as shown in Fig.2. In the condensed arrangement, conductors are wound close to each other as the case would be in an electric machine winding. The impedance of each arrangement at four different access points is measured along the frequency range of interest. Access points represent the start and end terminals of the winding, in addition to the start of each layer.

III. Inductance in a Multiconductor System

Inductance is highly dependent on frequency. The penetration depth of the magnetic field inside various media is dependent on its frequency but also on properties of the medium being subjected to the field and penetrated namely the medium's conductivity and permittivity according to the following formula [3]:

$$\delta = \sqrt{\frac{1}{\pi f \mu \sigma}} \quad \ldots\ldots\ldots (1)$$

The 24-turn winding prototype is being modeled under FEMM magneto-static and time-harmonic magnetic analyses, in a way that application of static and quasi-static solvers is justified by maintaining the cross-sectional dimensions of the problem small compared to the wavelength of the analysis frequency. Given the converter output voltage rise time (t_r), and the electromagnetic wave propagation velocity in the conductor of interest ($v_{propagation}$), the wavelength corresponding to the critical conductor length ($\lambda_{critical}$) is expressed as below [5]:

$$\lambda_{critical} = t_r \cdot v_{propagation} \quad \ldots\ldots\ldots (2)$$

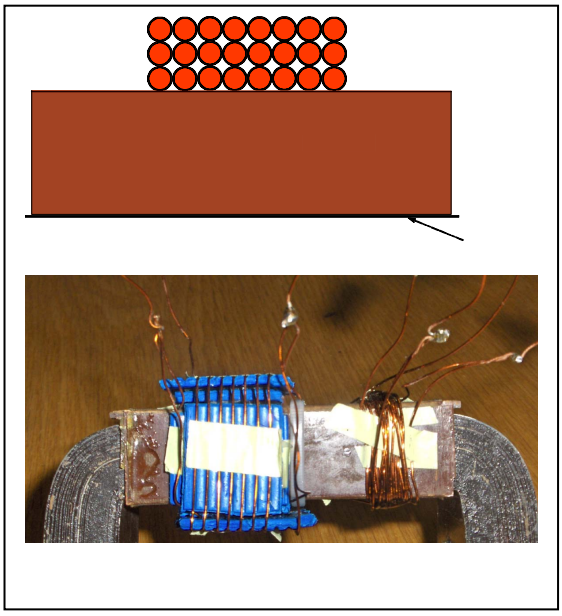

Fig. 2. The wiring arrangement of conductors for the FEMM analysis and in the prototype

A. FEMM Modeling Details

The prototype model for the condensed arrangements is modeled as 24 copper conductors in a 2D planar problem. The conductor and core depth inside the plane is 138 mm which is equivalent to one turn's length. The conductor diameter with insulation is 0.648 mm while copper diameter itself is 0.589 mm. Conductors are drawn with their insulation and placed close to each other where the center of conductors of different layers lie on the same vertical axis. They are numbered in an orderly manner as they are wound. See Fig.2. The bobbin, on which the winding is wound, is represented by a 3 mm high dielectric material above the iron core. Between the two ends of the unfolded core, an arc with a radius of 160 mm is drawn to represent the outer boundary limit that is assigned "mixed" boundary condition to model an unbounded problem [8]. Both ends of the core are configured with "Periodic"' boundary conditions to reflect that they are connected in reality and the resulting magnetic field will be the same at both of them. The top line of the core is configured with local element size that is dependent on the analysis frequency, and the bottom line is configured with a prescribed zero boundary condition where the magnetic vector potential (A) has a zero value. A screenshot of the described FEMM problem is shown in Fig.3.

B. The Analysis

The analysis is performed by assigning each conductor a circuit property of a current value of 1 Ampere, while the rest of conductors are assigned circuit properties of zero current values. The problem is solved for the *self-inductance* value for the conductor of concern, i.e. the one which has the stimulus current of 1 Ampere; meanwhile it is also solved for the *mutual*

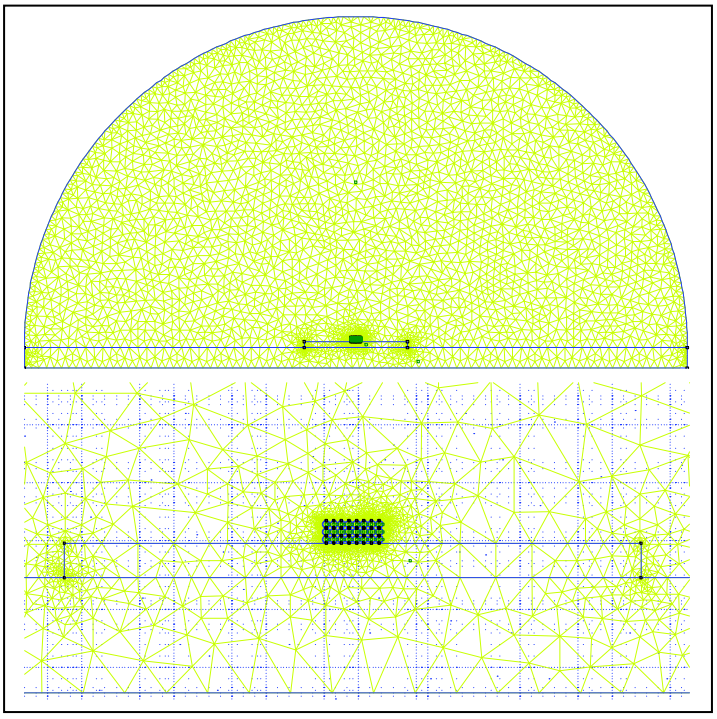

Fig. 3. One of the magneto-static analysis runs for the FEMM model of the winding arrangement on iron core prototype; A general meshed view of the problem (top), and a zoomed-in view (bottom)

inductance between the conductor of concern and every other conductor in the system during the same analysis run. For magneto-static problems, the analysis frequency is zero and so an unlimited theoretical penetration depth is considered as per equation (1). For AC time-harmonic magnetic problems, the analysis frequency is reflected by making the element size defining certain geometry, smaller than its corresponding magnetic-field penetration depth (δ), not least when drawing the iron core. The same goal can be also achieved by making the mesh size of a certain geometrical area smaller than its corresponding (δ).

C. The Outcome

Fig.4 shows the outcome of magneto-static analysis (top) and AC time-harmonic magnetic analysis at 2 kHz (bottom). Magnetic flux lines are shown inside the iron core; For magneto-static analysis the lines in the core represent the magnetic flux lines while in AC analysis, the lines represent the real part of the vector magnetic potential (A), as a complex number of (A) with both real and imaginary parts would result. It is noted that in the magneto-static case and also at "low" frequencies, the iron core acts as an attractive medium for the magnetic field flux lines to pass through, in order to complete their path, linking the current-carrying conductor to the core. This is due to the high permeability of the ferro-magnetic core at low frequencies, and the lamination thickness being smaller than the corresponding penetration depth. This contributes to higher values of inductance at low frequencies. As frequency increases for AC time-harmonic problems, the ferro-magnetic iron core tends to lose this flux-attraction feature. This is due to the associated core losses and the nonlinear behaviour of the iron magnetic permeability (μ_r) that affects the penetration depth of the magnetic field in iron at higher frequencies. This will cause the inductance to decrease with the frequency increase since the inductance is the magnetic flux divided by the current as in the relation:

$$\mathbf{L} = \frac{\Phi}{\mathbf{i}} \quad \text{..... (3)}$$

Due to skin effect, as frequency increases, the magnetic flux lines tend to have less penetration in the core laminations. There is a need to predict at which point/range the frequency starts to substantially influence the inductance, and to quantify how much that would be, compared to the dc or "low" frequency values for certain geometry and material characteristics. The ferro-magnetic core plays a very important role in this, since iron generally has the lowest penetration depth among other elements and metals, due to its high relative magnetic permeability (μ_r) that can range from 1000-9000 [4]. Penetration depth is inversely proportional to the magnetic permeability as per equation (1). In our case, according to the FEMM analysis, a substantial decrease in the inductance value to 15% lower than its corresponding dc value can be observed within the range of 300-400 Hz. Flux lines inside the core will gradually decrease beyond this frequency range until eventually, at very high frequencies, they tend to close their paths in the air with no need to pass through the iron core. Iron will effectively behave like air for very high-frequency magnetic fields.

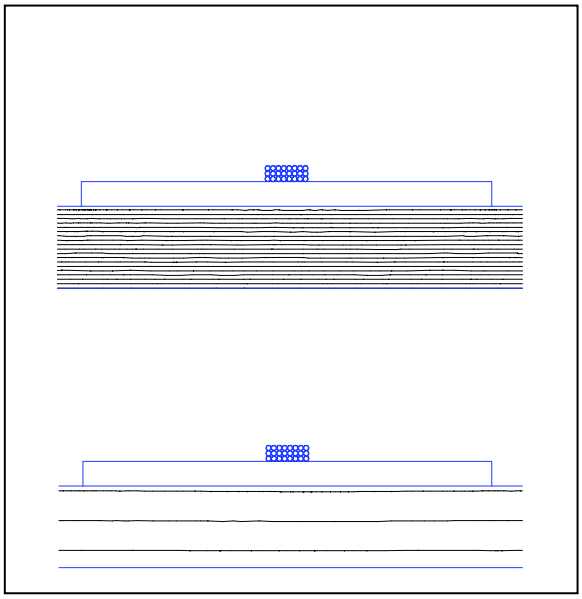

Fig. 4. Zoomed-in post-processor views of magneto-static and AC time-harmonic magnetic FEMM analyses, for the 24 conductors on core - condensed arrangement - at two extreme frequencies

IV. How the Inductive Coupling Matrix is Created?

For a given frequency, the FEMM model of the winding-on-core prototype has been run number of times equal to the number of conductors in the wiring arrangement. The reason being is that the stimulus current has been assigned to one conductor at a time to find the *self-inductance* and the *mutual-inductances* due to that stimulus, then, in the next run, the stimulus current is shifted to the neighboring conductor in the multi-conductor system. For each run this gives a number of results equal to the number of conductors in the system, i.e. 24 results in our case (1 *self-inductance* and 23 *mutual-inductance* values). This is repeated automatically until eventually creating a matrix system of 24 X 24 result values, in which the main diagonal elements represent the *self-inductance* and the off-diagonal elements represent the *mutual-inductance* values with symmetry and redundancy around the main diagonal as can be seen in Fig.5 where a 3D plot and a 2D images of the *Inductive Coupling Matrix* is shown. The FEMM analysis frequency is 0 Hz (dc). For other frequency analysis values, the resulting inductance will be a complex-number where the imaginary component expresses the core losses.

V. Complex-Numbered Inductance Concept

From equation (3) when the magnetic flux lags the current in time-harmonic problems, due to core losses of eddy currents and hysteresis, it will result in complex-numbered inductance of which the imaginary part is a lumped representation of the core losses. When **L** is the complex-numbered inductance, it is written as:

$$\mathbf{L} = \mathbf{L_r} - \mathbf{jL_i} \quad \text{..... (4)}$$

Where L_r is the real part of the inductance, L_i is the imaginary

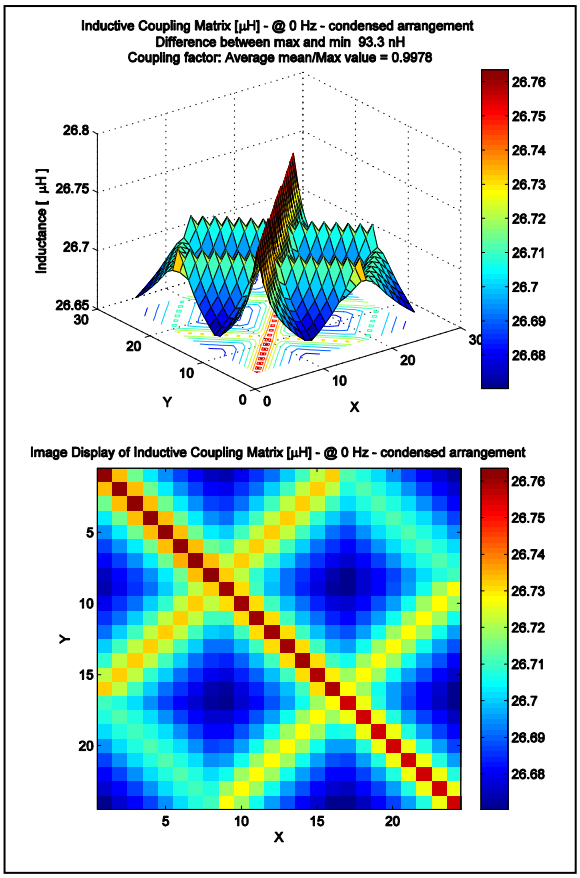

Fig. 5. Linear scale representation of *Inductive Coupling Matrix* run at 0 Hz frequency for the system of 24 conductors on iron core

part. Considering the impedance of inductance to be $Z(\omega) = j\omega L$, where ω is the angular frequency in [rad/s]. We have:

$$\mathbf{Z(\omega) = j\omega L_r + \omega L_i} \quad \ldots\ldots\ldots (5)$$

The imaginary part of **L** contributes to a real part of the frequency-dependent impedance $\mathbf{Z(\omega)}$, associated with core losses. One could interpret the (ωL_i) term as a frequency-dependent resistance which will be used later to develop a circuit model for the core losses along a frequency sweep. The real part of **L** contributes to the imaginary part of $\mathbf{Z(\omega)}$ which is associated with inductive energy storage.

VI. MEASUREMENTS

The inductance measurements vs frequency is shown in Fig.6. Inductance measurements have been produced after complex conversion from s-parameters of the input-port reflection coefficient Γ_{in}. Measurements indicate that a single turn inductance in the arrangement is about 2.5 μH at 1 kHz. Simulation results gave 6 μH at 1 kHz. This difference is due to capacitances between the turns and error in the value of the iron relative magnetic permeability (μ_r) used.

VII. CONCLUSIONS

A complex-numbered *Inductive Coupling Matrix* has been created to express a certain wiring arrangement. This is achieved by automatically running a MATLAB® code

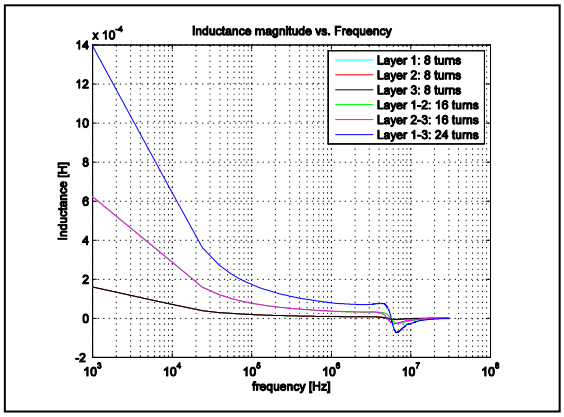

Fig. 6. Inductance measurements for the different layers of the prototype

employing Lua Script Language to generate a desired geometry, solve it under magneto-static analysis and AC time-harmonic analyses of different frequency values, and then perform some post-processing manipulations to get the *self-* and *mutual- inductances* and save them in a matrix format.

The *Inductive coupling matrix* is a basic ingredient in the RLC transmission line model of the stator slot. It contributes to a broadband CM-model of the electric machine which can be used in a circuit simulation environment to predict high-frequency CM current.

REFERENCES

[1] F. Abdallah. EMC Analysis of Electric Drives. Licentiate Dissertation, Tryckeriet i E-huset, Lund University, Lund 2012.

[2] J. Adabi, F. Zare, G. Ledwich, and A. Ghosh. Leakage current and common mode voltage issues in modern ac drive systems. In Power Engineering Conference, 2007. AUPEC 2007. Australasian Universities, pages 1 −6, December 2007.

[3] D. K. Cheng. Field and Wave Electromagnetics. Addison-Wesley series in electrical engineering. Addison-Wesley, 1989.

[4] Cogent Typical Data. Non-oriented electrical steel, June 2012. Surahammars Bruks AB, PO Box 201, SE-735 23 Surahammar, Sweden.

[5] J. Luszcz. Motor cable effect on the converter fed ac motor common-mode current. In Compatibility and Power Electronics (CPE), 2011 7th International Conference-Workshop, pages 445 −450, June 2011.

[6] J. Luszcz and K. Iwan. Conducted EMI propagation in inverter-fed ac motor. In Electrical Power Quality and Utilisation Magazine, Vol II, No. 1, pages 47 − 51, 2006. 2

[7] O. Magdun, A. Binder, C. Purcarea, and A. Rocks. High-frequency induction machine models for calculation and prediction of common-mode stator ground currents in electric drive systems. In Power Electronics and Applications, 2009. EPE '09. 13th European Conference on, pages 1 −8, September 2009.

[8] D. Meeker. Finite Element Method Magnetics - User's Manual, Version 4.2. dmeeker@ieee.org, October 2010.

[9] V. Mihaila, S. Duchesne, and D. Roger. A simulation method to predict the turn-to-turn voltage spikes in a PWM fed motor winding. Dielectrics and Electrical Insulation, IEEE Transactions on, 18(5):1609−1615, October 2011.

[10] N. Mohan, T. M. Undeland, and W. P. Robbins. Power Electronics: Converters, Applications and Design. Wiley, New York, 1995.

[11] S. Ogasawara and H. Akagi. Modeling and damping of high-frequency leakage currents in PWM inverter-fed ac motor drive systems. IEEE Transactions on Industry Applications, 32(5):1105 - 1114, September-October 1996.

[12] B.W. Williams. Principles and Elements of Power Electronics: Devices, Drivers,Applications and Passive Components. Barry W Williams, 2006.